

## Effect of Cu–Sn intermetallic compound reactions on the Kirkendall void growth characteristics in Cu/Sn/Cu microbumps

This content has been downloaded from IOPscience. Please scroll down to see the full text.

2014 Jpn. J. Appl. Phys. 53 05HA06

(<http://iopscience.iop.org/1347-4065/53/5S3/05HA06>)

View [the table of contents for this issue](#), or go to the [journal homepage](#) for more

Download details:

IP Address: 74.65.166.64

This content was downloaded on 02/07/2014 at 20:13

Please note that [terms and conditions apply](#).

## Effect of Cu–Sn intermetallic compound reactions on the Kirkendall void growth characteristics in Cu/Sn/Cu microbumps

Jong-Myeong Park<sup>1</sup>, Seung-Hyun Kim<sup>1</sup>, Myeong-Hyeok Jeong<sup>2</sup>, and Young-Bae Park<sup>1\*</sup>

<sup>1</sup>School of Materials Science and Engineering, Andong National University, Andong, Gyeongbuk 760-749, Korea

<sup>2</sup>NEPES Corporation, Cheongwon, Chungbuk 363-883, Korea

E-mail: ybpark@andong.ac.kr

Received October 9, 2013; accepted February 24, 2014; published online April 28, 2014

Growth behaviors of intermetallic compounds (IMCs) and Kirkendall voids in Cu/Sn/Cu microbump were systematically investigated by an in-situ scanning electron microscope observation. Cu–Sn IMC total thickness increased linearly with the square root of the annealing time for 600 h at 150 °C, which could be separated as first and second IMC growth steps. Our results showed that the growth behavior of the first void matched the growth behavior of second  $\text{Cu}_6\text{Sn}_5$ , and that the growth behavior of the second void matched that of the second  $\text{Cu}_3\text{Sn}$ . It could be confirmed that double-layer Kirkendall voids growth kinetics were closely related to the Cu–Sn IMC growth mechanism in the Cu/Sn/Cu microbump, which could seriously deteriorate the mechanical and electrical reliabilities of the fine-pitch microbump systems. © 2014 The Japan Society of Applied Physics

### 1. Introduction

Three-dimensional (3D) integrated circuits (ICs) have advantages of decreased power consumption, excellent electrical properties, and high form-factor performance. The newest electronic packaging technology in the form of vertical stack bonding of interconnected device layers is required to develop 3D ICs.<sup>1–8</sup> Flip-chip packaging technology has been widely used in the electronics industry in recent years as high performance and miniaturized electronics have become more common. However, solder bumps are limited to applications with a fine pitch of less than 100  $\mu\text{m}$  due to the bump bridging between adjacent bumps.<sup>9–11</sup> Therefore, fine-pitch Cu/solder/Cu microbump structure has been developed to overcome this limitation.<sup>12</sup> Electrical reliability can also be improved with this structure because the Cu pillars of the Cu/Sn/Cu microbump have superior electrical and thermal conductivities.<sup>13</sup> However, because the Cu/Sn/Cu microbump is made of a typical Sn-rich solder between Cu pillars, metallurgical reactions can lead to the formation of layered Cu–Sn intermetallic compounds (IMC), namely  $\text{Cu}_6\text{Sn}_5$  and  $\text{Cu}_3\text{Sn}$ , on the pad surface. Right after reflow,  $\text{Cu}_3\text{Sn}$  layer is usually extremely thin, while both IMCs grow subsequently by solid-state reactive diffusion processes. Although Cu–Sn IMCs are essential for the formation of robust solder joints, such solder joints with Cu–Sn IMCs are often susceptible to Kirkendall voiding, which induces premature mechanical failures of electronic packages.<sup>14,15</sup> The voids grown under thermal aging conditions (e.g., under Cu–Sn IMC growth or under accelerated thermal aging) can lead to the mechanical weakening of the solder joints, which can cause failures in subsequent shock tests or in the extreme case, even under the stresses associated with thermal cycling.<sup>16</sup> IMC growth kinetics and Kirkendall void formation in conventional solder bumps have been subjects of extensive experimental and theoretical studies.<sup>17–21</sup> To our knowledge, however, experimental evidences on the effect of IMC kinetics on Kirkendall void growth characteristics have not been systematically investigated.<sup>22,23</sup> It was reported for conventional solder bump structure that segregation of residual S atoms to form new  $\text{Cu}_3\text{Sn}/\text{Cu}$  interface, Kirkendall voiding, and phase transformation from  $\text{Cu}_6\text{Sn}_5$  to  $\text{Cu}_3\text{Sn}$  can be repeated under extensive aging conditions, which led to form multiple

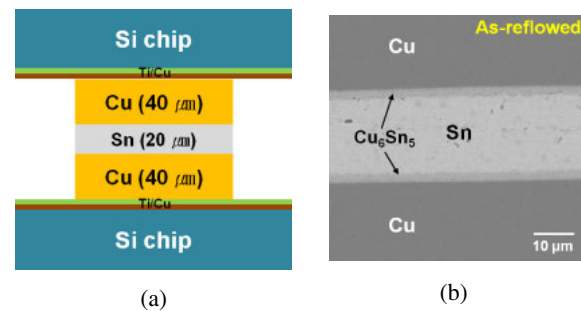
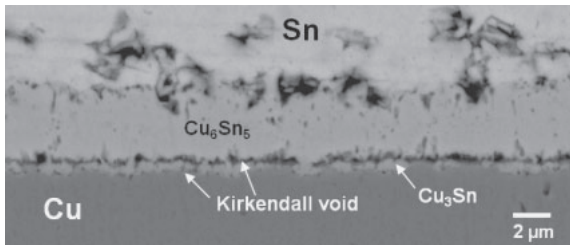


Fig. 1. (Color online) As-reflowed Cu/Sn/Cu microbump structure: (a) schematic diagram, and (b) cross-sectional SEM image.

layers of Kirkendall voids.<sup>24</sup> However, little systematic and quantified analyses has been carried out on the relationship between IMC phase growth kinetics and Kirkendall void growth characteristics in Cu/Sn microbump systems. In this paper, IMCs and Kirkendall void growth kinetics in Cu/Sn/Cu microbumps during annealing were correlated each other by in-situ SEM observations and quantification.

### 2. Experimental procedure

Figure 1 shows a schematic diagram and cross-sectional scanning electron microscope (SEM) image of the Cu/Sn/Cu microbump structure used in this study. In order to fabricate this specimen, Ti (50 nm) and Cu (200 nm) layers were sputtered subsequently on a Si substrate to act as the adhesion layer and the seed layer, respectively. Subsequently, a dry film photoresist was used for lithographic processing to open a space with height of 50  $\mu\text{m}$  over 80  $\mu\text{m}$  diameter. Cu pillars were made by using an electroplated 40- $\mu\text{m}$ -thick Cu layer and an electroplated 10- $\mu\text{m}$ -thick pure Sn layer. The diameters of the Cu pillars were 80  $\mu\text{m}$ . Pure Sn solders at both the top chip and bottom chip were directly interconnected during the bonding process. Bonding pressure of 24 MPa was applied during bonding on hot plate in the vacuum chamber. The bonding temperature was 280 °C, and the bonding time was maintained for 1 min at the peak temperature. After bonding, the final Sn thickness was determined to be around 20  $\mu\text{m}$ . To observe real-time IMCs



**Fig. 2.** Enlarged BSE micrographs of the cross-sectioned Cu/Sn/Cu interface annealed for 100 h at 150 °C.

growth behaviors as a function of annealing time, the cross-section of the sample was ground with #2000 SiC paper and then polished using a diamond suspension (1–3 μm). The IMC thickness and Kirkendall void area were quantified by an in-situ method: Cu/Sn/Cu microbump with 20-μm-thick Sn layer was annealed in an SEM chamber at 150 °C. The growth of IMCs and Kirkendall voids between Sn/Cu interfaces was analyzed by using SEM back-scattered electron (BSE) mode and by energy-dispersive X-ray spectroscopy (EDS). The Cu–Sn IMCs and voids were quantified using an image analyzer where IMC thickness was defined as the area of IMC divided by the interface length.

### 3. Results and discussion

In order to investigate in-situ evolution of the interfacial microstructure and the growth characteristics of Cu–Sn IMCs in Cu/Sn/Cu microbumps during annealing, SEM BSE images were taken of the cross-sectioned microbumps with annealing time, as shown in Fig. 2 for 100 h at 150 °C. SEM and EDS results suggested that only Cu<sub>6</sub>Sn<sub>5</sub> was present at the Sn/Cu interfaces right after bonding, and that Cu<sub>3</sub>Sn and Kirkendall voids formed and grew at the Cu<sub>6</sub>Sn<sub>5</sub>/Cu interface with increasing annealing time. Figure 3 shows the cross-sectional BSE images and schematic diagrams at Cu/Sn interfaces during annealing at 150 °C. After bonding for 1 min at 280 °C, the interfacial Sn and Cu phases reacted to form Cu<sub>6</sub>Sn<sub>5</sub> phase immediately at Cu/Sn interface, and the Cu<sub>3</sub>Sn phase nucleated near interface between the Cu<sub>6</sub>Sn<sub>5</sub> and Cu pillar during annealing. The Cu<sub>3</sub>Sn/Cu interface was void-free before annealing, but Kirkendall voids began to nucleate at the interface during annealing.<sup>24)</sup> After 50 h annealing at 150 °C, the first Kirkendall voids fully covered the Cu<sub>3</sub>Sn/Cu interface, as shown in Fig. 3(b). The island-type second Cu<sub>3</sub>Sn IMC started to form inside Cu after 150 h. After 150 h annealing, Cu<sub>3</sub>Sn above the first Cu<sub>3</sub>Sn/Cu interface coalesced completely, and subsequent Sn diffusion into the Cu pillar through the remaining ligament of the interface formed islands of second Cu<sub>3</sub>Sn denoted as inside the Cu pillar,<sup>24)</sup> as shown in Fig. 3(c). The first Cu<sub>3</sub>Sn/Cu interface was replaced by the Cu<sub>6</sub>Sn<sub>5</sub>/Cu interface after 150 h annealing. With further annealing, the second Cu<sub>3</sub>Sn thickened and two noteworthy phenomena occurred. First, Kirkendall voids nucleated at the new second Cu<sub>3</sub>Sn/Cu interface after annealing. Second, the initially straight Cu<sub>6</sub>Sn<sub>5</sub>/Cu interface was replaced by a thick first Kirkendall void interface, as shown in Fig. 3(d). Similarly with the previous reports on the multiple voiding phenomena for conventional solder bump structure,<sup>20,24)</sup> as the second

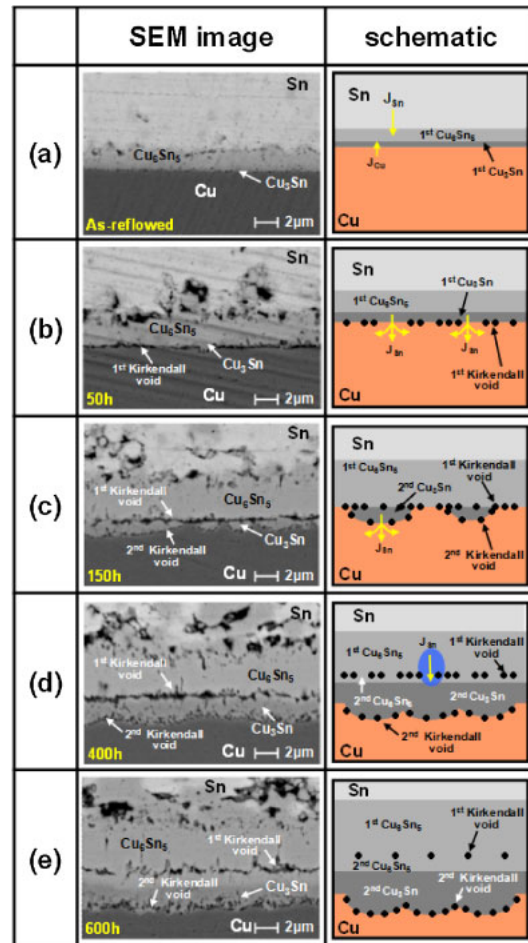


**Fig. 3.** (Color online) In-situ SEM images and schematic diagrams of Cu/Sn/Cu microbump annealed at 150 °C for various times; (a) 0, (b) 50, (c) 150, (d) 400, and (e) 600 h.

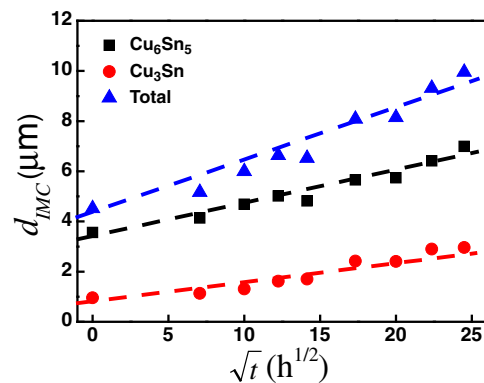


**Fig. 4.** (Color online) Thickness variations of Cu–Sn IMC phases with annealing time at 150 °C.

Cu<sub>3</sub>Sn/Cu interface was continuously covered by the Kirkendall voids that grew at the new interface, the flux of Cu atoms into Cu<sub>3</sub>Sn was again inhibited and the second Cu<sub>6</sub>Sn<sub>5</sub> started to form, replacing the second Cu<sub>3</sub>Sn between the first and second Kirkendall voids,<sup>24)</sup> as shown in Fig. 3(e). To understand the differences in IMC growth kinetics, the thicknesses of Cu<sub>6</sub>Sn<sub>5</sub> and Cu<sub>3</sub>Sn IMCs are shown in Fig. 4 as a function of annealing time at 150 °C. Total thickness of each IMC increased linearly with the

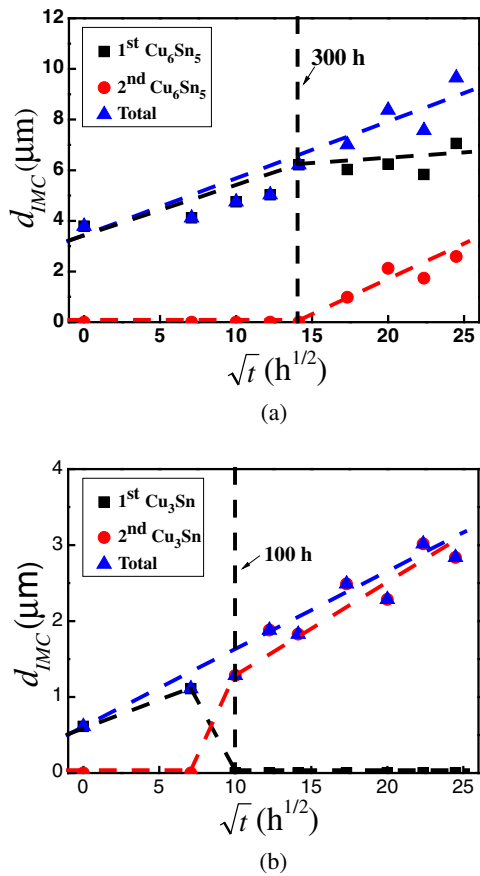


Fig. 5. (Color online) Thickness variations of each separated IMC phase with annealing time at 150 °C: (a) Cu<sub>6</sub>Sn<sub>5</sub> and (b) Cu<sub>3</sub>Sn.

square root of the annealing time, which implies that the IMC growth was controlled by the diffusion mechanism. However, in the case of the separated Cu<sub>6</sub>Sn<sub>5</sub>, the first Cu<sub>6</sub>Sn<sub>5</sub> marginally grew after 300 h and at the same time, the second Cu<sub>6</sub>Sn<sub>5</sub> grew below the first Kirkendall voids, as shown in Fig. 5(a). The first Cu<sub>3</sub>Sn linearly increased before 100 h but was rapidly consumed after 100 h. Also, the second Cu<sub>3</sub>Sn IMC started to form in the Cu pillar after 100 h, as shown in Fig. 5(b). This means that even though the Cu<sub>3</sub>Sn/Cu interface appeared to have been fully covered with Kirkendall voids after 50 h, a substantial portion of the interface remained connected [cf. Fig. 3(b)], which served as a path for matter diffusion, similarly with the previous reports for conventional solder bump structure.<sup>24)</sup> Figure 6 shows the Kirkendall void area of the first void and second void as a function of the square root of the annealing time at 150 °C. The void growth velocities of the first void decreased after 300 h at 150 °C, while the second void started to form after 100 h at 150 °C. These results showed the reasonable correlations not only between the first voids and second Cu<sub>6</sub>Sn<sub>5</sub> growth behavior, but also between the second voids and second Cu<sub>3</sub>Sn growth behavior, as shown in Fig. 7. As the initial Cu<sub>3</sub>Sn/Cu interfaces moved to the Cu pillar side, voids flux decreased from the Cu pillar. In our previous work, it was confirmed that the growth kinetics of Kirkendall void area was very closely related to the Cu<sub>3</sub>Sn IMC growth kinetics.<sup>25)</sup> Second voids grew as the initial Cu<sub>3</sub>Sn/Cu interface moved to the second interface (Cu pillar side). By

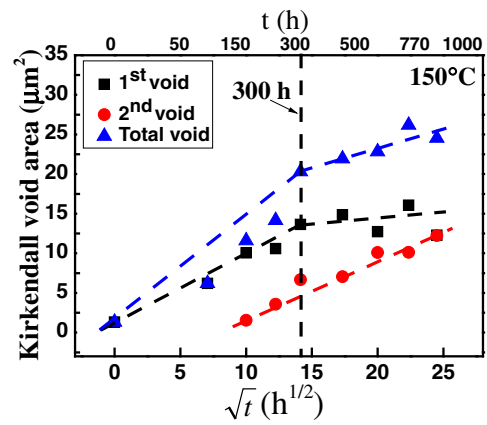


Fig. 6. (Color online) Variations of Kirkendall void area with annealing time at 150 °C.

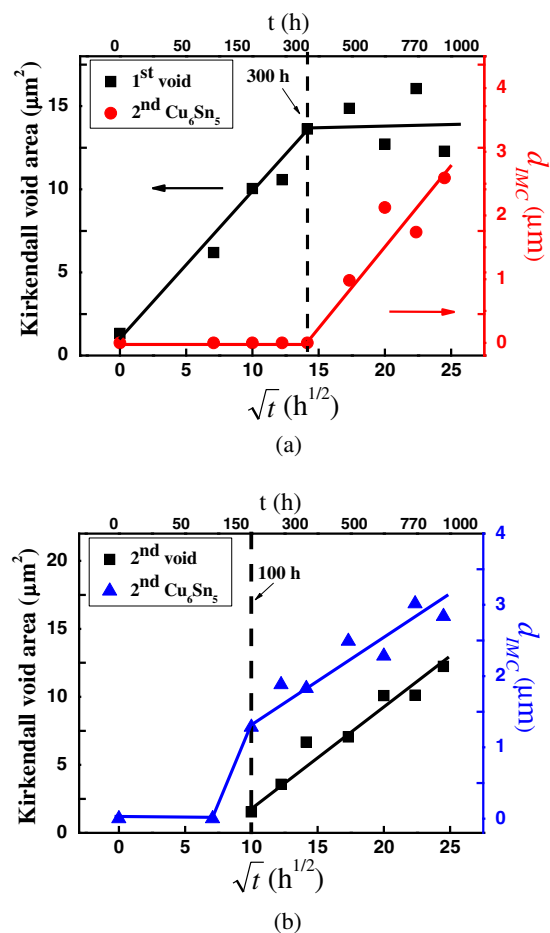


Fig. 7. (Color online) Correlation between Kirkendall void area and Cu-Sn IMC thickness with annealing time at 150 °C: (a) first Kirkendall void and second Cu<sub>6</sub>Sn<sub>5</sub>, and (b) second Kirkendall voids and second Cu<sub>3</sub>Sn.

repeating this process, double-layers Kirkendall voids were formed between the first Cu<sub>6</sub>Sn<sub>5</sub> and the remaining Cu pillar, as shown in Fig. 3(e). Kim et al.<sup>24)</sup> reported that IMCs and Kirkendall voids of multiple layers were observed in a conventional solder bump. Such behaviors were also observed in the Cu/Sn/Cu microbump and it could be confirmed that double-layer Kirkendall void growth kinetics were closely related to the second IMC growth mechanism.

More detail studies on the effects of multiple-layer Kirkendall voids growth on the mechanical and electrical reliabilities of the fine-pitch microbump systems are necessary.

#### 4. Conclusions

Quantitative correlations between Cu–Sn IMCs growth and Kirkendall voids growth kinetics in Cu/Sn/Cu microbumps were systematically investigated using in-situ SEM observations during annealing at 150 °C. Thicknesses of total Cu<sub>6</sub>Sn<sub>5</sub> and Cu<sub>3</sub>Sn phases followed a linear relationship with the square root of the annealing time. The first Kirkendall void growth rate matched the second Cu<sub>6</sub>Sn<sub>5</sub> growth rate, while the second voids growth rate matched the second Cu<sub>3</sub>Sn growth rate. Double-layer Kirkendall void growth mechanism were closely related to the second IMC growth mechanism in the Cu/Sn/Cu microbump, which could affect the mechanical and electrical reliabilities of the fine-pitch microbump systems.

#### Acknowledgements

This research was supported by Nano Material Technology Development Program (Green Nano Technology Development Program) through the National Research Foundation of Korea (NRF) funded by the Ministry of Education, Science and Technology (MEST) (2011-0019986), and also by Basic Science Research Program through NRF funded by MEST (2011-0015023). The authors would like to thank Professor Hoo-Jeong Lee and Dr. Byoung Hoon Lee at Sungkyunkwan University for sample fabrication and fruitful discussion.

- 1) B. H. Kwak, M. H. Jeong, and Y. B. Park, *Korean J. Met. Mater.* **50**, 775 (2012) [in Korean].
- 2) W. Yao and C. Basaran, *Electron. Mater. Lett.* **8**, 503 (2012).

- 3) J. Jun, J. K. Park, and J. P. Jung, *Met. Mater. Int.* **18**, 487 (2012).
- 4) E. Choi, H. S. Choi, A. Kim, S. J. Lee, Y. Cui, S. H. Kwon, C. H. Kim, S. J. Hahn, H. Son, and S. G. Pyo, *Met. Mater. Int.* **19**, 1339 (2013).
- 5) Z. Wu, Z. Huang, Y. Ma, H. Xiong, and P. P. Conway, *Electron. Mater. Lett.* **10**, 281 (2014).
- 6) S. Kumar, S. Mallik, N. Ekere, and J. Jung, *Met. Mater. Int.* **19**, 1083 (2013).
- 7) S. C. Hong, S. Kumar, D. H. Jung, W. J. Kim, and J. P. Jung, *Met. Mater. Int.* **19**, 123 (2013).
- 8) Y.-J. Lee, H.-W. Yeon, S.-Y. Jung, S.-K. Na, J.-S. Park, Y.-Y. Choi, H.-J. Lee, O.-S. Song, and Y.-C. Joo, *Electron. Mater. Lett.* **10**, 275 (2014).
- 9) K. S. Kim, Y. C. Lee, J. H. Ahn, J. Y. Song, C. D. Yoo, and S. B. Jung, *Korean J. Met. Mater.* **48**, 1028 (2010) [in Korean].
- 10) M. Y. Kim, T. S. Oh, and T. S. Oh, *Korean J. Met. Mater.* **48**, 557 (2010) [in Korean].
- 11) S. H. Huh, K. D. Kim, K. S. Kim, and J. S. Jang, *Electron. Mater. Lett.* **8**, 59 (2012).
- 12) K. L. Lin, E. Y. Chang, and L. C. Shih, *Microelectron. Eng.* **86**, 2392 (2009).
- 13) J. M. Kim, J. S. Park, and K. T. Kim, *Met. Mater. Int.* **16**, 657 (2010).
- 14) K. Zeng, R. Stierman, T. C. Ciu, D. Edwards, K. Ano, and K. N. Tu, *J. Appl. Phys.* **97**, 024508 (2005).
- 15) C. E. Ho, T. T. Kuo, C. C. Wang, and W. H. Wu, *Electron. Mater. Lett.* **8**, 495 (2012).
- 16) L. Yin, P. Kondos, P. Borgesen, Y. Liu, S. Bliznakov, F. Wafula, N. Dimitrov, D. W. Henderson, C. Parks, M. Gao, J. Therriault, J. Wang, and E. Cotts, *Proc. 59th Electronic Components and Technology Conf.*, 2009, p. 406.
- 17) B. J. Kim, G. T. Lim, J. D. Kim, K. W. Lee, Y. B. Park, H. Y. Lee, and Y. C. Joo, *J. Electron. Mater.* **39**, 2281 (2010).
- 18) K. N. Tu and R. D. Thompson, *Acta Metall.* **30**, 947 (1982).
- 19) Z. Mei, M. Ahmad, M. Hu, and G. Ramakrishna, *Proc. 55th Electronic Components and Technology Conf.*, 2005, p. 415.
- 20) J. Y. Kim and J. Yu, *Appl. Phys. Lett.* **92**, 092109 (2008).
- 21) M. Date, K. N. Tu, T. Shoji, M. Fujiyoshi, and K. Sato, *J. Mater. Res.* **19**, 2887 (2004).
- 22) W. Yang, R. W. Messler, Jr., and L. E. Felton, *J. Electron. Mater.* **23**, 765 (1994).
- 23) T. Laurila, V. Vourinen, and J. K. Kivilahti, *Mater. Sci. Eng. R* **49**, 1 (2005).
- 24) S. H. Kim and J. Yu, *J. Mater. Res.* **25**, 1854 (2010).
- 25) G. T. Lim, B. J. Kim, K. W. Lee, J. D. Kim, Y. C. Joo, and Y. B. Park, *J. Electron. Mater.* **38**, 2228 (2009).